

See discussions, stats, and author profiles for this publication at: <https://www.researchgate.net/publication/279937638>

Garnet–spinel–olivine–orthopyroxene equilibria in the FeO–MgO–Al₂O₃–SiO₂–Cr₂O₃ system: I. Composition and molar volumes of minerals

Article in *European Journal of Mineralogy* · July 1999

CITATIONS

52

READS

321

4 authors, including:



Gerhard Peter Brey

Goethe-Universität Frankfurt am Main

235 PUBLICATIONS 9,700 CITATIONS

SEE PROFILE



Alexander Ivanovich Turkin

Sobolev Institute of Geology and Mineralogy

25 PUBLICATIONS 264 CITATIONS

SEE PROFILE

Some of the authors of this publication are also working on these related projects:



deep mantle inclusions [View project](#)



Carbonatites REE in-situ analysis [View project](#)

Garnet-spinel-olivine-orthopyroxene equilibria in the FeO-MgO-Al₂O₃-SiO₂-Cr₂O₃ system: I. Composition and molar volumes of minerals

GERHARD P. BREY¹, ALEXEI M. DOROSHEV^{2†}, ANDREI V. GIRNIS^{1,3}
and ALEXANDR I. TURKIN²

¹Institut für Mineralogie, J.W. Goethe-Universität, Senckenberganlage 28,
D-60054 Frankfurt am Main, Germany. – e-mail: brey@em.uni-frankfurt.de

²Institute of Mineralogy and Petrography, Universitetskii pr. 3, Novosibirsk 630090, Russia
[†]Deceased

³Institute for Geology of Ore Deposits, 35 Staromonetny, Moscow 109017, Russia

Abstract: Experiments in the FMASCr system at pressures of 30–50 kbar and temperatures of 1200–1500°C model mineral equilibria in depleted mantle harzburgite. Special emphasis was on the partitioning of chromium between garnet, spinel and orthopyroxene and the influence of chromium on the garnet to spinel peridotite transition. The experiments were carried out using mixtures of synthetic minerals as starting materials with different initial compositions of phases, approaching the conditions of reversed experiments. The equilibrium between minerals was attained rapidly with respect to Fe-Mg exchange, whereas a considerable scatter in Cr/(Cr+Al) values was observed in all phases studied. The extreme compositions of phases in reversed experiments give insight on the equilibrium phase composition. Cr/(Cr+Al) ratio of garnet coexisting with orthopyroxene, olivine and spinel increases with pressure and temperature, exceeding 0.4 at 50 kbar and 1500°C. At high pressure spinel becomes also more chromian, while orthopyroxene composition approaches the enstatite-ferrosilite join. After quench, the minerals were studied by X-ray diffraction in order to obtain unit-cell parameters of solid solutions and refine their volume properties. Spinel in the system (Mg, Fe)(Cr, Al)₂O₄ show negative deviation from ideal mixing volume at high Cr contents and positive deviation in Al-rich composition (Margules excess mixing volume parameters: $W_{CrAl} = 0.017$ and $W_{AlCr} = -0.007$ J/bar). Small negative excess volume of mixing is related to Fe-Mg mixing in spinel. Cr-Al mixing in garnet is characterised by a small excess mixing volume, which may be approximated by a symmetrical model ($W_{AlCr}^V = W_{CrAl}^V = 0.018$ J/bar). Our results are compatible with zero excess mixing volume of orthopyroxene solid solution. All the excess volumes of mixing are small and their influence on equilibria is substantial only at very high pressures (> 50 kbar).

Key-words: phase equilibrium, molar volume, solid solution, mantle mineralogy, peridotite.

Introduction

As a major component in some mantle phases (spinel, garnet), chromium exerts a pronounced effect on phase associations in peridotite, especially on the stability of garnet and spinel assemblages. At higher pressures (> 40 kbar), garnet becomes the major host of chromium as demonstrated by high Cr contents in garnet from deep

xenoliths and inclusions in diamonds (Sobolev, 1974; Meyer, 1975). One of the possible Cr-bearing garnet end-members, uvarovite, Ca₃Cr₂Si₃O₁₂, is known to be stable at low and high pressures (Naka *et al.*, 1975). However, high-chromium mantle garnets generally contain too little calcium to accommodate all chromium as uvarovite. The existence of a new Fe-Mg Cr garnet has been proposed, with the end-members Mg₃Cr₂Si₃O₁₂, knor-

ringite (Nixon & Hornung, 1968) and $\text{Fe}_3\text{Cr}_2\text{Si}_3\text{O}_{12}$. The pure end-members have not been found in nature, but the mole fraction of knorringite in mantle garnet may be as high as 65% (Stachel & Harris, 1997). Experiments demonstrate the stability of Fe-Mg Cr garnets at high pressures, 60–100 kbar for knorringite (Ringwood, 1977; Irifune *et al.*, 1982; Turkin *et al.*, 1983; Doroshev *et al.*, 1997) and 60 kbar for $\text{Fe}_3\text{Cr}_2\text{Si}_3\text{O}_{12}$ (Fursenko, 1981). Cr in garnet may be a sensitive geobarometer for low-calcium mantle peridotites. The development of such a geobarometer is hampered by the lack of sufficiently accurate experimental data on the Cr-bearing mantle systems. The first experiments by Ringwood (1977) were concerned only with the synthesis of pure end-member knorringite, and those of Irifune *et al.* (1982) and Irifune & Hariya (1983) significantly overestimated pressure because pressure calibration was done only at room temperature. More accurate data on phase equilibria in the MASCr system were obtained by Doroshev *et al.* (1997), who studied the assemblages garnet-eskolaite-orthopyroxene and garnet-spinel-orthopyroxene-forsterite at pressures of 30–50 kbar and temperatures of 1200–1500°C. These authors provided phase diagrams for a model garnet-spinel harzburgite and estimated the conditions of crystallisation of high-chromium garnet included in diamonds. The influence of Ca and Fe on the distribution of chromium between coexisting phases was not taken into account. In harzburgite assemblages, only garnet contains appreciable amounts of calcium, and its influence may be estimated from the data on Ca-Mg-Fe mixing in garnet (Wood, 1988; Koziol & Newton, 1989; Berman *et al.*, 1995) and experiments in Cr-bearing lherzolitic systems (Webb & Wood, 1986; Nickel, 1986). The effect of iron is more difficult to assess, inasmuch as even the small amounts of iron typical of mantle peridotite may form iron-rich spinels which, in turn, may greatly affect the partitioning of chromium between spinel and garnet.

This work is part of an ongoing project aimed at the behaviour of chromium in the upper mantle under subsolidus conditions. Experiments in the system MASCr were reported by Doroshev *et al.* (1997), the present paper deals with the FMASCr system, and the study of calcium-bearing systems is under way. The goal of this study is to assess the mutual influence of Cr-Al and Fe-Mg substitution on the equilibria between garnet, spinel, orthopyroxene, and olivine.

Experimental methods

Starting materials

Doroshev *et al.* (1997) emphasised the importance of the adequate choice of starting materials for determining equilibrium composition of chromium-bearing minerals, because chromium diffusion in silicates is slow even at relatively high temperatures (*e.g.* Nickel, 1986). Similar to Doroshev *et al.* (1997), synthetic mineral mixtures were used with minerals of either high or low Cr/Al ratio to approach equilibrium from different directions. The minerals were synthesised from reagent-grade oxides under conditions described by Doroshev *et al.* (1997).

Since Fe and Mg equilibrate much faster than Cr and Al, only pure Fe or Mg phases were used (Table 1). We prepared six mixtures with two bulk compositions differing in their Cr/Al molar ratio (12:13 and 1:3). Mg/(Mg+Fe) ratio in all mixtures was set to be 0.9, but the resulting materials differed slightly from the target composition. Thus, the influence of Mg/(Mg+Fe) on the Cr-Al partitioning could be evaluated within a small compositional range. The pyrope that we used in our starting mixtures contained approximately 0.5 wt.% CaO because of small Ca contents in magnesite used for synthesis. This resulted in <0.15 wt.% of CaO in the bulk compositions of starting mixtures with this mineral. Garnets, especially in the runs with low modal garnet, contained up to 2 wt.% of CaO, which is equivalent to 4 mol.% of the uvarovite end-member. This calcium admixture in garnets was accounted for in further evaluation of the composition data. Among other phases only orthopyroxene contained detectable amounts of CaO in some experiments (up to 0.15–0.35 wt.%).

In each experiment three different mixtures were used simultaneously (Table 1). Chemical equilibrium was approached from different directions: in mixtures (A) and (D) garnet would gain Cr from spinel at experimental conditions, and spinel would become more Al-rich by uptake of Al from garnet; orthopyroxene takes in both Al and Cr. Approach to equilibrium in mixtures (B) and (E) was from Cr-bearing garnet, pure spinel and enstatite. Mixtures (C) and (F) were designed to reverse orthopyroxene composition, because the amount of Cr and Al in the starting orthopyroxene was much higher than the solubility of these elements at experimental conditions. Use of different iron-bearing phases in these mixtures

allowed us to judge equilibration with respect to Fe-Mg exchange.

Experimental set-up

Three starting mixtures separated by graphite discs were loaded into a graphite container, which was welded into a Pt capsule with 4 mm inner diameter. The double graphite-platinum capsule provides oxygen fugacity at or below the graphite-CO-CO₂ equilibrium, which is located above the iron-wuestite buffer under the experimental conditions (Thompson & Kushiro, 1972; Woermann & Rosenhauer, 1985). Accordingly, no metal phase appeared, and ferric iron content was negligible in all phases.

The experiments were carried out with a belt apparatus at the Max-Planck-Institut für Chemie, Mainz, which was recently transferred to the University of Frankfurt. The belt apparatus was calibrated by Brey *et al.* (1990), and P and T are believed to be accurate within $\pm 7^\circ$ and 0.5 kbar. The experimental temperature and pressure conditions were varied between 1200 and 1500°C and 30 and 50 kbar, with run durations from 2.5 (1500°C) to 7 days (1200°C) (Table 1).

The experimental products were examined by optical microscopy and analysed by powder X-ray diffractometry and electron microprobe.

X-ray diffraction patterns were recorded using a Philips X-ray powder diffractometer system ARD-15 with CuK α radiation in the range $17^\circ < 2\theta < 70^\circ$ at a counter rate of $0.5^\circ \text{ min}^{-1}$. High-purity silicon was used as an internal standard (cell edge $a_0 = 5.43088 \text{ \AA}$). Silicon was added in an amount that permitted fixing the doublets α_1 and α_2 of its least intense reflection (400). Correction was determined by the three reflections that did not overlap with the reflections of the phases studied. If the scatter of the correction determined by these reflections did not exceed 0.01° (2θ) the average was taken as the correction value, otherwise the correction was calculated as a linear function of the 2θ angle. The unit-cell parameters of synthesised phases were calculated using the least squares method.

Experimental charges were cut and polished for electron microprobe analysis with the Cameca (Camebax Microbeam) electron microprobe of the Institut für Geowissenschaften, Universität Mainz, equipped with a Kevex energy-dispersive system. The accelerating voltage was 15 kV, the beam cur-

Table 1. Experimental conditions and run products.

Run	Mixture ^a	Pressure (kbar)	T(°C)	Duration (h)	Run products
789/4	D	30	1200	168	Ol, Opx, Sp, Grt
789/5	E	30	1200	168	Ol, Opx, Sp, Grt
789/6	F	30	1200	168	Ol, Opx, Sp, Grt
69/4	D	30	1300	86	Ol, Opx, Sp, Grt
69/5	E	30	1300	86	Opx, Sp, Grt
69/6	F	30	1300	86	Ol, Opx, Sp, Grt
67/4	D	30	1400	64	Ol, Opx, Sp, Grt
67/5	E	30	1400	64	Opx, Sp, Grt
67/6	F	30	1400	64	Ol, Opx, Sp, Grt
70/4	D	30	1500	46	Ol, Opx, Sp
70/5	E	30	1500	46	Ol, Opx, Sp, Grt
70/6	F	30	1500	46	Ol, Opx, Sp, Grt
71/1	A	40	1200	138	Ol, Opx, Sp, Grt
71/2	B	40	1200	138	Ol, Opx, Sp, Grt
71/3	C	40	1200	138	Ol, Opx, Sp, Grt
68/1	A	40	1300	96	Ol, Opx, Sp, Grt
68/2	B	40	1300	96	Ol(?), Opx, Sp, Grt
68/3	C	40	1300	96	Ol, Opx, Sp, Grt
66/1	A	40	1400	98	Ol, Opx, Sp, Grt
66/2	B	40	1400	98	Ol(?), Opx, Sp, Grt
66/3	C	40	1400	98	Ol, Opx, Sp, Grt
65/1	A	40	1500	62	Ol, Opx, Sp, Grt
65/2	B	40	1500	62	Ol(?), Opx, Sp, Grt
65/3	C	40	1500	62	Ol, Opx, Sp, Grt
788/1	A	50	1200	143	Ol, Opx, Sp, Grt
788/2	B	50	1200	143	Ol, Opx, Sp, Grt
788/3	C	50	1200	143	Ol, Opx, Sp, Grt
72/1	A	50	1300	119	Ol, Opx, Sp, Grt
72/2	B	50	1300	119	Ol, Opx, Sp, Grt
72/3	C	50	1300	119	Ol, Opx, Sp, Grt
792/1	A	50	1400	110	Ol, Opx, Sp, Grt
792/2	B	50	1400	110	Ol, Opx, Sp, Grt
792/3	C	50	1400	110	Ol, Opx, Sp, Grt
787/1	A	50	1500	64	Ol, Opx, Sp, Grt
787/2	B	50	1500	64	Ol, Opx, Sp, Grt
787/3	C	50	1500	64	Ol, Opx, Sp, Grt

^a Minerals in starting mixtures:

A - Pyr+Fa+En+Pc+Fo; B - Pyr₄₀Kn₆₀+Alm+Fo+En+Sp

C - Pyr₄₀Kn₆₀+Fo+Fa+Herc+En₈₀Crts₂₀

D - Pyr+Fa+En+Pc+Fo; E - Pyr₅₀Kn₅₀+Alm+Fo+En+Sp

F - Pyr₅₀Kn₅₀+Fo+Herc+En₈₀Crts₂₀

Bulk composition of starting mixtures:

A, B, C - Pyr₄₂Kn₄₈Alm₁₀+Fo₉₀Fa₁₀

D, E, F - Pyr₆₅Kn₂₅Alm₁₀+Fo₉₀Fa₁₀

rent 20 nA, the counting time 100 s, and the beam size 2 μm . Pure metals and oxides were used as standards and ZAF correction procedures were after Reed & Ware (1975). The experimental phases were normally between 10 and 20 μm in size. In most cases the outer parts of grains were analysed. Five to ten analyses were carried out for each phase.

Table 2. Average composition and unit-cell parameters of experimental olivines.

Run	SiO ₂	FeO	MgO	Cr ₂ O ₃	Total	mg# ^a	a, Å ^b	b, Å	c, Å	V, Å ³
789/6	38.92	12.30	45.92	1.03	98.17	0.869				
69/4	40.76	7.50	50.80	0.56	99.60	0.924	4.7626(7)	10.2242(7)	5.9909(5)	291.72(4)
69/6	39.59	12.21	46.89	0.61	99.30	0.872				
67/4	39.57	7.68	50.24	0.98	98.46	0.921				
67/6	38.30	12.71	45.42	2.36	98.79	0.864				
70/4	40.29	7.84	50.47	0.83	99.41	0.920	4.7604(4)	10.2191(8)	5.9931(5)	291.55(3)
68/1	40.11	7.02	50.92	1.01	99.06	0.928				
66/1	40.92	7.01	52.37	0.73	101.03	0.930				
65/1	40.56	7.34	50.87	1.10	99.87	0.925				
788/1	40.26	6.14	51.75	0.42	98.57	0.938	4.7588(5)	10.2229(12)	5.9974(6)	291.77(4)
788/3	40.01	7.82	48.41	0.96	97.20	0.917	4.7632(2)	10.2241(7)	5.9894(4)	291.68(2)
72/1	40.86	6.31	51.91	0.66	99.74	0.936	4.7628(4)	10.215(1)	5.9876(8)	291.32(5)
72/3	40.32	7.41	50.99	0.79	99.50	0.925	4.7623(5)	10.223(1)	5.9903(7)	291.62(4)
792/1	40.38	6.53	51.43	0.76	99.09	0.934	4.7618(4)	10.222(9)	5.9873(5)	291.43(3)
792/2	41.85	4.51	54.27	0.79	101.42	0.955	4.760(1)	10.208(1)	5.9867(7)	290.87(5)
792/3	40.50	7.69	50.79	0.97	99.95	0.922	4.7629(4)	10.218(1)	5.9902(5)	291.52(3)
787/1	40.39	7.11	50.85	1.22	99.56	0.927	4.7638(6)	10.2179(9)	5.9882(8)	291.48(4)
787/2	41.02	5.17	52.62	1.05	99.86	0.948	4.7584(8)	10.215(1)	5.988(13)	291.07(6)
787/3	40.40	9.00	49.44	1.78	100.62	0.907	4.7652(3)	10.2239(9)	5.9919(4)	291.92(2)

^a mg# = Mg/(Mg+Fe) ^b Figures in parentheses are standard deviation (1σ) in units of the last digit.

Mineral composition

In the majority of the experiments the desired four-phase association was observed in the run products (Table 1). Only at 30 kbar and 1500°C garnet was absent in mixture (D) and olivine was not found in the experimental products from 30 kbar and 1300 and 1400°C with mixture (E). Tables 2–5 show the results, which include average and the most advanced compositions with respect to Cr/(Cr+Al) ratio.

Olivine

Mg/(Mg+Fe) ratios of olivine are generally uniform and highest in the run products with starting mixtures (B) and (E) (Table 2) (0.94–0.96), lowest in those with (C) and (F) mixtures (0.87–0.92), and intermediate with mixtures (A) and (D) (0.92–0.93). Olivine is high in chromium (0.4–2.4 wt.% as Cr₂O₃) which displays considerable scatter. Chromium oxidation state was not determined in olivine or any other phase. Chromium contents in olivine is much higher than found in natural samples <0.5 wt.% Cr₂O₃, see Meyer, 1975). This suggests a significant fraction of Cr₂SiO₄, whose solubility in olivine at the experimental pressure and temperature is very high (5–25 mol.%) (Li *et al.*, 1995). In a similar set of

experiments Engi (1983) found tiny inclusions of Cr spinel in olivine, which were only visible under an electron microscope.

Spinel

In most cases spinel is close to the (Mg,Fe²⁺)(Cr,Al)₂O₄ solid solution. Recalculation of the slight deviation from ideal stoichiometry results in positive and “negative” Fe³⁺ contents of 0.02 to –0.02 evenly distributed around 0. This is within the errors of microprobe analysis, which indicates that Fe³⁺ content is negligible.

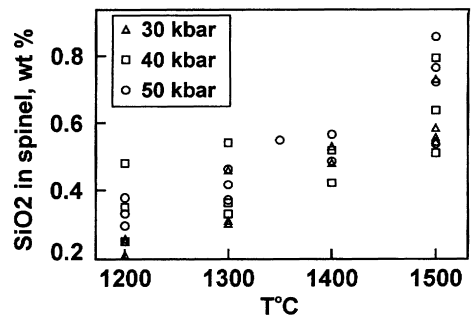


Fig. 1. Concentration of SiO₂ in experimental spinels as a function of temperature.

Table 3. Average composition (wt.%), compositional ratios and unit-cell parameters of experimental spinels.

Run	SiO ₂	Al ₂ O ₃	FeO	MgO	Cr ₂ O ₃	Total	mg# ^a	cr# ^b	min cr#	max cr#	a, Å
789/4	0.21	27.15	10.44	17.02	44.32	99.14	0.77(7)	0.47(21)	0.373	0.896	8.190(1)
789/5	0.21	37.55	6.34	20.76	33.50	98.36	0.863(7)	0.37(2)	0.356	0.401	8.1872(5)
789/6	0.25	38.95	11.30	17.74	30.50	98.73	0.71(7)	0.36(19)	0.122	0.579	8.214(2)
69/4	0.31	36.19	8.41	19.46	34.18	98.55	0.81(1)	0.39(3)	0.349	0.433	8.1812(5)
69/5	0.31	39.06	6.50	20.84	31.96	98.67	0.855(3)	0.36(1)	0.335	0.370	8.177(4)
69/6	0.46	37.11	11.94	17.48	32.32	99.31	0.72(3)	0.36(4)	0.329	0.421	8.183(2)
67/4	0.57	41.13	8.39	20.35	28.33	98.76	0.83(1)	0.31(3)	0.274	0.367	8.1735(3)
67/5	0.46	40.93	6.14	21.30	29.58	98.40	0.862(7)	0.325(5)	0.323	0.334	8.1755(4)
67/6	0.41	29.51	9.83	17.40	40.98	98.13	0.799(4)	0.257(9)	0.245	0.264	8.1930(6)
70/4	0.55	42.04	7.66	20.82	27.98	99.06	0.836(8)	0.31(1)	0.291	0.323	8.1750(4)
70/5	0.54	42.10	6.01	21.80	27.68	98.12	0.876(3)	0.305(3)	0.303	0.310	8.1711(4)
70/6	0.78	37.31	10.97	18.24	31.67	98.98	0.751(4)	0.37(1)	0.335	0.376	8.1914(7)
71/1	0.25	12.78	11.36	14.57	60.62	99.58	0.68(2)	0.74(3)	0.733	0.817	8.2786(5)
71/2	0.45	15.29	7.90	16.90	58.08	98.61	0.77(1)	0.717(4)	0.713	0.724	8.2725(4)
71/3	0.59	13.01	16.10	11.76	57.21	98.66	0.56(1)	0.75(1)	0.733	0.758	8.2801(5)
68/1	0.29	14.01	10.70	15.13	58.95	99.08	0.70(2)	0.75(4)	0.696	0.773	8.2640(4)
68/2	0.65	17.20	8.02	17.40	55.59	98.87	0.79(1)	0.684(3)	0.682	0.689	8.2657(4)
68/3	0.54	16.36	11.33	15.11	55.63	98.97	0.694(9)	0.69(2)	0.675	0.729	8.2694(4)
66/1	0.52	19.15	10.21	16.84	53.13	99.85	0.752(9)	0.65(1)	0.642	0.668	8.2556(5)
66/2	0.59	18.33	8.01	17.65	54.67	99.24	0.786(8)	0.666(3)	0.664	0.670	8.2615(3)
66/3	0.52	18.67	11.43	15.22	52.55	98.39	0.697(9)	0.64(2)	0.637	0.692	8.2595(2)
65/3	0.79	20.88	12.25	15.70	49.58	99.20	0.699(4)	0.614(2)	0.612	0.618	8.2507(4)
65/2	0.59	19.60	6.60	18.42	53.59	98.79	0.816(6)	0.646(2)	0.646	0.649	8.2512(4)
65/1	0.64	19.46	9.68	16.87	52.73	99.39	0.751(6)	0.646(2)	0.641	0.647	8.2534(4)
788/1	0.30	7.85	11.63	13.48	66.07	99.34	0.654(8)	0.85(1)	0.831	0.864	8.3012(5)
788/2	0.38	10.58	8.00	16.11	63.50	98.56	0.759(4)	0.797(8)	0.796	0.815	8.2927(4)
788/3	0.33	9.64	13.16	12.86	63.16	99.15	0.62(1)	0.81(1)	0.797	0.829	8.3025(4)
72/1	0.37	10.41	11.02	14.86	62.96	99.61	0.70(1)	0.79(2)	0.785	0.839	8.2910(3)
72/2	0.42	12.27	7.80	16.87	61.06	98.41	0.786(8)	0.77(1)	0.760	0.788	8.2847(5)
72/3	0.46	11.86	12.01	14.60	59.66	98.58	0.688(4)	0.771(3)	0.769	0.776	8.2923(5)
792/1	0.59	8.67	11.53	14.84	65.39	101.03	0.692(8)	0.835(2)	0.833	0.838	8.3045(4)
792/2	0.61	9.33	8.39	16.32	64.35	99.00	0.760(6)	0.822(2)	0.820	0.826	8.2991(3)
792/3	0.57	8.82	12.32	14.21	63.08	99.00	0.67(1)	0.828(1)	0.826	0.829	8.3082(2)
787/1	0.72	10.48	10.88	15.08	62.57	99.72	0.701(6)	0.801(2)	0.798	0.803	8.2936(4)
787/2	0.77	11.23	8.02	16.71	62.27	98.99	0.770(5)	0.788(2)	0.786	0.790	8.2890(4)
787/3	0.86	10.72	12.90	14.15	60.93	99.56	0.656(3)	0.792(1)	0.791	0.793	8.2980(4)

^a mg# = Mg/(Mg+Fe), all iron as FeO. Median values; figures in parentheses are standard deviation in units of the last digit.

^b cr# = Cr/(Cr+Al). Median values; figures in parentheses are standard deviation in units of the last digit.

In contrast to the MASCr system (Doroshev *et al.*, 1997), spinel analyses from the experiments in the FMASCr system show 0.2 to 0.8 wt.% of SiO₂ (Table 3). The SiO₂ contents could be due to microinclusions of silicates, however, the clear positive correlation with temperature (Fig. 1) suggests silica dissolution in the spinel structure.

The Cr/(Cr+Al) ratio of spinel ranges from 0.25 to 0.87, increasing with pressure (Fig. 2). Negative temperature dependence of this ratio at constant pressure is also apparent. Mg/(Mg+Fe) ratios of spinel are much lower and vary widely

(0.53–0.88 within the whole experimental range) as compared with olivine.

At all pressures and temperatures the Mg/(Mg+Fe) ratio of spinel is rather uniform in any experiment, ranging normally within ± 0.005 (Fig. 2). At high temperatures (1400–1500°C) the Cr/(Cr+Al) ratio is also very uniform (± 0.01 or less). At 1200–1300°C and especially at 30 kbar, this interval is much larger (0.03–0.3). No simple correlation exists between the direction of approach to equilibrium and the composition of spinels (Fig. 2). The spinels in the runs with chro-

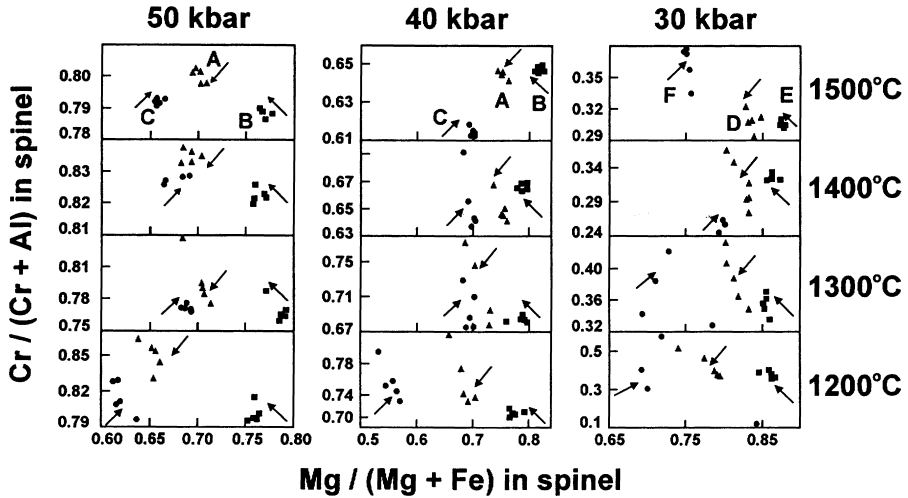


Fig. 2. Composition of experimental spinels from harzburgite mineral assemblages at different pressures and temperatures. All microprobe analyses are shown. Spinel compositions from experiments with various starting mixtures are shown by different symbols: triangles - (A) and (D) (30 kbar); squares - (B) and (E) (30 kbar); circles - (C) and (F) (30 kbar). Arrows show the assumed changes in mineral composition during equilibration.

mian spinel in the starting material may be either higher or lower with respect to their $\text{Cr}/(\text{Cr}+\text{Al})$ ratio compared to the charges from the same experiments with initially aluminous spinel. No definite correlation was observed between $\text{Mg}/(\text{Mg}+\text{Fe})$ and $\text{Cr}/(\text{Cr}+\text{Al})$ ratios at constant pressure and temperature. Usually, $\text{Cr}/(\text{Cr}+\text{Al})$ ratios in the three charges of any experiment were very similar in spite of quite different initial spinel compositions.

Garnet

The majority of experimental garnets yielded a slight excess of the sum of cations (8.01–8.03) when calculated on the basis of 12 oxygens. This excess lies within the error of microprobe analysis, but, if real, would imply 0.02–0.06 Fe^{3+} p.f.u. Although it correlates (negatively) with temperature and pressure, the deviation from stoichiometry does not depend on iron content of garnet which could be expected if this deviation were due to Fe^{3+} incorporation. Because of the uncertainties, we ignored the possible presence of ferric iron and expressed the relationship of trivalent cations in garnet with a single parameter, $\text{Cr}/(\text{Cr}+\text{Al})$. Garnets from the experiments with mixtures (A) and (D) contain up to 1.5–2 wt.% CaO (Table 4),

which corresponds to a $\text{Ca}/(\text{Ca}+\text{Mg}+\text{Fe})$ ratio in garnet of 0.03–0.04.

Garnet is the most iron-rich of the coexisting silicates. Its $\text{Mg}/(\text{Mg}+\text{Fe})$ value is normally 0.92–0.94 for experiments with mixtures (B) and (E), 0.88–0.9 for (A) and (D), and 0.84–0.9 for (C) and (F). This ratio increases slightly with temperature but not with pressure. Normally, the experimental garnets are uniform with respect to their $\text{Mg}/(\text{Mg}+\text{Fe})$ ratios; these vary within ± 0.005 at 1400 and 1500°C and ± 0.01 in the lower-temperature experiments (Fig. 3).

The $\text{Cr}/(\text{Cr}+\text{Al})$ ratio is less uniform (Fig. 3). Even at 1500°C the range of $\text{Cr}/(\text{Cr}+\text{Al})$ values is as large as 0.1–0.2 (Table 4). The most chromian garnets were produced in the experiments at 50 kbar and 1500°C ($\text{Cr}/(\text{Cr}+\text{Al}) > 0.4$). The Cr contents of garnets decrease rapidly with decreasing pressure and temperature, and the $\text{Cr}/(\text{Cr}+\text{Al})$ ratio is below 0.1 in the experiments at 30 kbar and 1200–1300°C (Fig. 3).

Orthopyroxene

Orthopyroxenes from the experiments are close to ideal stoichiometry with sums of cations ranging from 3.99 to 4.01 calculated for 6 oxygens. CaO content of orthopyroxenes is normally below

Table 4. Average compositions (wt.%), compositional parameters, and cell edges of experimental garnets.

Run	SiO ₂	FeO	MgO	Al ₂ O ₃	Cr ₂ O ₃	CaO	Total	mg# ^a	cr# ^b	min cr#	max cr#	a, Å
789/4	41.95	6.12	24.36	22.30	2.84	1.78	99.34	0.88(2)	0.07(1)	0.059	0.105	11.4744(7)
789/5	43.20	3.87	27.58	23.38	2.38	0.10	100.52	0.926(6)	0.06(2)	0.039	0.088	11.4722(6)
789/6	41.85	7.59	24.53	22.43	2.69	0.00	99.09	0.853(6)	0.074(4)	0.070	0.081	11.479(1)
69/4	42.29	5.18	25.48	22.66	2.76	1.20	99.57	0.898(2)	0.09(2)	0.036	0.091	11.491(1)
69/5	42.55	4.51	26.71	22.29	3.40	0.17	99.63	0.92(1)	0.095(6)	0.083	0.096	11.4764(6)
69/6	42.26	8.88	24.22	22.25	2.78	0.03	100.42	0.85(2)	0.08(2)	0.051	0.096	11.474(1)
71/1	42.17	6.01	24.97	20.48	5.03	0.82	99.49	0.89(1)	0.13(4)	0.092	0.186	11.4760(7)
71/2	42.05	3.74	26.61	18.35	8.43	0.23	99.41	0.927(2)	0.22(5)	0.180	0.342	11.4922(6)
71/3	41.38	8.20	23.61	19.59	6.39	0.16	99.33	0.835(7)	0.18(1)	0.165	0.192	11.4935(8)
68/1	41.48	5.17	24.96	19.79	6.18	0.86	98.43	0.896(2)	0.18(4)	0.116	0.222	11.5012(8)
68/2	42.22	3.89	26.67	19.02	7.85	0.10	99.75	0.924(3)	0.21(1)	0.205	0.233	11.4986(5)
68/3	42.01	5.76	25.44	20.61	5.59	0.09	99.51	0.88(1)	0.14(8)	0.075	0.282	11.4960(7)
66/1	42.04	4.97	25.18	19.50	6.91	1.32	99.92	0.900(2)	0.20(4)	0.129	0.239	11.501(1)
66/2	42.07	3.81	26.65	18.03	9.09	0.22	99.88	0.924(2)	0.24(3)	0.228	0.292	11.4982(3)
66/3	41.94	5.51	25.48	19.66	6.91	0.15	99.65	0.87(2)	0.24(4)	0.130	0.220	11.4951(7)
65/3	41.81	6.59	24.68	17.75	9.12	0.18	100.13	0.897(9)	0.26(8)	0.171	0.425	11.5041(5)
65/2	41.66	3.35	26.62	17.66	10.12	0.22	99.63	0.935(3)	0.28(3)	0.241	0.322	11.5020(5)
65/1	41.62	4.97	25.13	18.28	8.45	0.90	99.35	0.900(3)	0.237(7)	0.228	0.245	11.496(1)
788/1	41.47	5.81	24.34	18.98	6.96	1.18	98.75	0.88(1)	0.21(4)	0.131	0.241	11.495(1)
788/2	41.78	3.22	26.72	18.40	8.21	0.11	98.45	0.93(1)	0.23(5)	0.135	0.333	11.4956(6)
788/3	41.22	5.89	24.49	16.54	10.22	0.11	98.49	0.87(3)	0.2(2)	0.105	0.584	11.5000(6)
72/1	41.51	5.11	24.98	17.64	8.84	0.75	98.83	0.899(7)	0.26(2)	0.229	0.282	11.5080(6)
72/2	41.46	3.51	26.58	18.02	9.31	0.11	98.99	0.931(2)	0.25(2)	0.248	0.290	11.5008(3)
72/3	41.53	5.01	25.57	17.77	8.95	0.17	98.99	0.89(2)	0.25(2)	0.238	0.287	11.5032(7)
792/1	41.63	5.13	24.92	14.62	13.17	0.67	100.13	0.897(1)	0.37(1)	0.360	0.395	11.5244(5)
792/2	41.63	3.53	26.18	15.17	12.41	0.09	99.01	0.929(3)	0.36(1)	0.339	0.378	11.5160(4)
792/3	40.96	5.55	24.75	15.05	12.37	0.14	98.83	0.888(1)	0.35(1)	0.329	0.366	11.5201(4)
787/1	40.92	5.22	24.61	14.54	12.87	0.60	98.76	0.893(2)	0.38(3)	0.321	0.394	11.5264(5)
787/2	41.15	3.82	25.67	12.90	15.38	0.33	99.26	0.925(4)	0.38(11)	0.336	0.591	11.5186(3)
787/3	41.22	6.50	24.27	14.43	13.01	0.06	99.48	0.869(5)	0.38(4)	0.333	0.436	11.5225(4)

^a mg# = Mg/(Mg+Fe+Ca), all iron as FeO. Median values; figures in parentheses are standard deviation in units of the last digit.

^b cr# = Cr/(Cr+Al). Median values; figures in parentheses are standard deviation in units of the last digit.

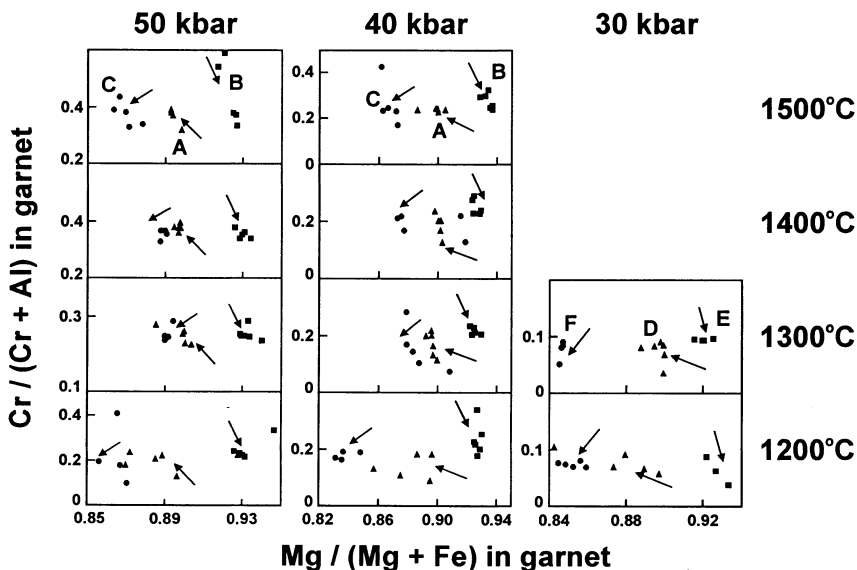


Fig. 3. Compositions of experimental garnets. See Fig. 2 for symbol explanation.

Table 5. Average compositions (wt.%), compositional parameters, and cell edges of experimental orthopyroxenes.

Run	SiO ₂	Al ₂ O ₃	FeO	MgO	CaO	Cr ₂ O ₃	Total	mg# ^a	Cr ^b	min Cr	max Cr	Al ^b	min Al	max Al	a, Å ^c	b, Å	c, Å	V Å ³
789/4	55.72	4.55	5.39	33.85	0.31	1.19	101.00	0.914(8)	0.031(3)	0.030	0.036	0.19(1)	0.167	0.190	18.232(1)	8.7927(6)	5.1882(3)	831.72(6)
789/5	55.21	5.28	3.10	34.94	n.d.	1.41	99.94	0.953(3)	0.040(5)	0.030	0.041	0.22(2)	0.181	0.230	18.2179(8)	8.7793(4)	5.1851(3)	829.31(3)
789/6	53.94	4.66	7.18	32.12	n.d.	2.10	100.01	0.87(3)	0.06(1)	0.048	0.080	0.18(2)	0.170	0.215				
69/4	53.54	6.02	4.58	33.10	0.34	1.75	99.33	0.927(2)	0.048(3)	0.044	0.050	0.246(5)	0.241	0.251	18.2259(8)	8.7840(5)	5.1890(3)	830.75(5)
69/5	54.36	5.84	3.49	34.22	n.d.	1.68	99.60	0.946(2)	0.047(8)	0.035	0.055	0.25(3)	0.183	0.272	18.2156(7)	8.7708(5)	5.1879(3)	828.84(5)
69/6	54.39	4.97	6.32	32.63	n.d.	2.16	100.48	0.92(2)	0.06(1)	0.037	0.081	0.20(4)	0.133	0.240	18.228(1)	8.7969(6)	5.1893(6)	832.12(9)
67/4	53.24	6.39	4.74	32.91	0.22	1.69	99.18	0.925(3)	0.045(3)	0.045	0.051	0.264(8)	0.252	0.271	18.2235(8)	8.77728(4)	5.1893(3)	830.03(5)
67/5	52.63	7.97	3.51	33.26	n.d.	2.30	99.67	0.944(1)	0.060(5)	0.056	0.068	0.32(2)	0.292	0.335	18.2097(6)	8.7628(4)	5.1888(2)	827.96(4)
67/6	54.94	3.81	5.52	33.24	n.d.	2.27	99.77	0.92(1)	0.07(1)	0.048	0.078	0.16(3)	0.107	0.189				
70/4	53.39	6.82	4.76	32.81	0.24	1.99	100.01	0.925(3)	0.055(4)	0.048	0.059	0.28(2)	0.226	0.304	18.2192(7)	8.7739(4)	5.1906(2)	829.74(4)
70/5	52.38	8.28	3.54	33.20	n.d.	2.38	99.77	0.944(2)	0.064(1)	0.063	0.066	0.336(8)	0.324	0.345	18.2087(8)	8.7628(5)	5.1886(2)	827.89(5)
70/6	51.87	6.83	6.78	30.90	n.d.	2.88	99.26	0.890(5)	0.08(1)	0.068	0.099	0.27(4)	0.245	0.346	18.2222(9)	8.7858(4)	5.1920(3)	831.23(5)
71/1	56.68	2.50	4.36	35.16	0.17	1.40	100.27	0.935(4)	0.038(1)	0.036	0.040	0.09(2)	0.091	0.129	18.239(1)	8.8076(5)	5.1842(3)	832.82(6)
71/2	56.52	2.50	2.67	36.20	n.d.	1.65	99.54	0.959(2)	0.045(1)	0.043	0.046	0.101(4)	0.094	0.104				
71/3	54.69	3.23	6.31	32.87	n.d.	2.35	99.44	0.90(1)	0.07(1)	0.046	0.078	0.13(4)	0.094	0.175	18.2371(9)	8.8115(6)	5.1877(3)	833.64(6)
68/1	55.90	2.66	4.17	34.95	0.19	1.68	99.54	0.937(1)	0.048(6)	0.036	0.051	0.11(1)	0.092	0.118	18.2347(9)	8.8048(4)	5.1870(2)	832.79(5)
68/2	56.28	3.17	3.01	35.51	n.d.	2.11	100.08	0.954(1)	0.059(4)	0.052	0.060	0.127(5)	0.122	0.135	18.2319(9)	8.7991(4)	5.1866(3)	832.06(6)
68/3	55.29	3.18	4.90	33.98	n.d.	2.40	99.75	0.924(4)	0.07(1)	0.051	0.074	0.12(2)	0.106	0.163	18.240(1)	8.8029(6)	5.1862(4)	832.73(7)
66/1	55.93	3.42	4.24	34.57	0.24	2.19	100.58	0.935(2)	0.060(2)	0.056	0.061	0.138(5)	0.132	0.142	18.2352(8)	8.8000(4)	5.1871(3)	832.37(5)
66/2	56.04	3.70	3.18	35.22	n.d.	2.43	100.57	0.952(2)	0.065(1)	0.064	0.066	0.148(2)	0.146	0.150	18.226(1)	8.7908(6)	5.1851(4)	830.74(7)
66/3	55.75	2.81	5.43	33.88	n.d.	2.24	100.10	0.917(2)	0.062(6)	0.053	0.067	0.11(1)	0.092	0.135	18.2371(9)	8.8029(4)	5.1888(3)	833.01(6)
65/3	54.15	3.48	6.30	34.08	n.d.	2.26	100.26	0.908(3)	0.063(7)	0.054	0.069	0.16(2)	0.108	0.165				
65/2	55.10	4.14	2.91	34.89	n.d.	2.91	99.96	0.955(1)	0.079(5)	0.074	0.087	0.166(3)	0.164	0.171	18.2280(8)	8.7908(4)	5.1879(3)	831.30(5)
65/1	55.72	3.26	4.44	34.27	0.28	2.37	100.34	0.933(1)	0.062(6)	0.060	0.074	0.14(1)	0.116	0.147	18.2356(8)	8.8026(4)	5.1910(3)	833.26(5)
788/1	57.06	1.45	4.01	35.33	0.15	1.38	99.39	0.942(7)	0.035(8)	0.030	0.051	0.062(7)	0.051	0.066	18.239(1)	8.8144(7)	5.1859(5)	833.69(8)
788/2	57.48	1.65	2.54	36.89	n.d.	1.52	100.07	0.962(2)	0.040(4)	0.035	0.048	0.065(5)	0.062	0.075	18.232(1)	8.8111(4)	5.1852(4)	832.98(6)
788/3	56.08	2.01	4.39	34.80	n.d.	1.84	99.12	0.930(8)	0.05(1)	0.031	0.068	0.07(3)	0.054	0.150	18.237(1)	8.8216(7)	5.180(1)	833.3(1)
72/1	56.58	1.84	4.08	34.87	0.19	1.73	99.29	0.94(1)	0.04(1)	0.036	0.076	0.08(2)	0.040	0.099	18.238(1)	8.8087(7)	5.1854(4)	833.03(7)
72/2	57.00	2.12	2.62	36.34	n.d.	1.79	99.88	0.960(2)	0.047(5)	0.044	0.056	0.085(2)	0.083	0.088	18.229(1)	8.8054(5)	5.1834(3)	832.02(6)
72/3	56.18	2.09	4.67	34.62	n.d.	1.79	99.36	0.931(4)	0.049(3)	0.045	0.054	0.086(8)	0.072	0.097	18.239(1)	8.8056(6)	5.1872(3)	833.08(6)
792/1	57.03	1.44	3.89	35.12	0.15	1.69	99.32	0.942(2)	0.045(8)	0.038	0.060	0.060(6)	0.050	0.065	18.2378(1)	8.8146(7)	5.1834(4)	833.26(7)
792/2	58.16	1.66	2.81	36.71	n.d.	1.89	101.22	0.959(1)	0.050(2)	0.048	0.053	0.066(3)	0.061	0.069	18.2368(1)	8.8101(7)	5.1828(2)	832.70(6)
792/3	57.29	1.61	4.29	35.28	n.d.	1.67	100.14	0.936(2)	0.045(1)	0.044	0.046	0.065(1)	0.064	0.066	18.247(2)	8.8026(8)	5.1878(4)	833.3(1)
787/1	56.49	1.98	4.37	34.58	0.16	2.18	99.76	0.934(2)	0.059(5)	0.053	0.066	0.079(3)	0.078	0.086	18.238(2)	8.8117(9)	5.1860(5)	833.4(1)
787/2	57.00	2.06	3.12	35.65	n.d.	2.30	100.13	0.953(2)	0.062(6)	0.052	0.068	0.084(9)	0.068	0.091	18.234(1)	8.8031(8)	5.1805(4)	831.54(8)
787/3	56.20	2.24	5.55	34.01	n.d.	2.23	100.22	0.916(1)	0.059(4)	0.057	0.067	0.089(5)	0.085	0.098	18.2386(1)	8.8173(7)	5.1865(4)	834.07(8)

^a mg# = Mg/(Mg+Fe), all iron as FeO. Median values; figures in parentheses are standard deviation in units of the last digit.

^b Median, maximum, and minimum Al and Cr are in formula unit on the basis of 6 O.

^c Figures in parentheses are standard deviation in units of the last digit.

n.d. - not determined, concentration below microprobe detection limit.

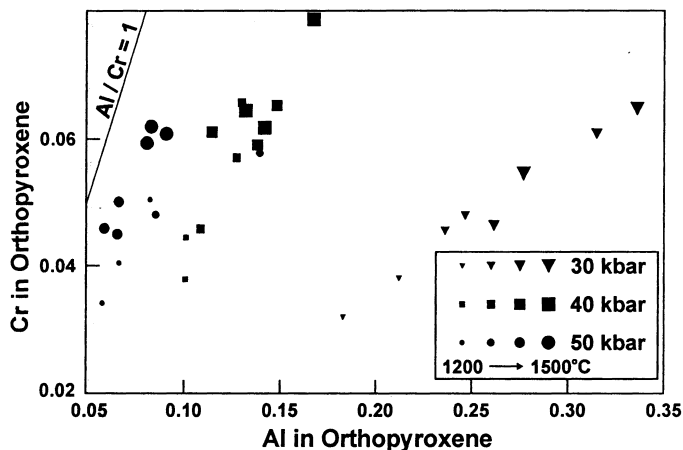


Fig. 4. Correlation of Al and Cr contents (formula units on the basis of 6 oxygen atoms) in orthopyroxene under different pressures. The size of symbols increases with experimental temperature, from 1200 to 1300, 1400, and 1500°C.

0.1 wt.%, and Al_2O_3 and Cr_2O_3 concentrations vary from 1.5 to 8.0 and from 1.0 to 6.5 wt.%, respectively (Table 5). The atomic fraction of Cr is always lower than that of Al (Fig. 4), suggesting that Cr enters orthopyroxene as the MgCrAlSiO_6 end-member. The distribution of aluminium between M1 and tetrahedral sites is thus given by: $\text{Al}_{\text{M1}} = (\text{Al}-\text{Cr})/2$ and $\text{Al}_{\text{T}} = (\text{Al}+\text{Cr})/2$. Bulk Al and Cr contents in orthopyroxene increase with temperature (Fig. 4). Increasing pressure strongly

reduces Al solubility in orthopyroxene, whereas the Cr content remains relatively constant (Fig. 4). The ratio $\text{Cr}/(\text{Cr}+\text{Al})$ increases strongly with pressure (from 0.14–0.24 at 30 kbar to 0.35–0.48 at 50 kbar) and is not very sensitive to temperature.

The $\text{Mg}/(\text{Mg}+\text{Fe})$ ratio of orthopyroxene is similar to that of olivine and remains within a very narrow interval in any sample including those from low temperature (1200–1300°C). Cr and

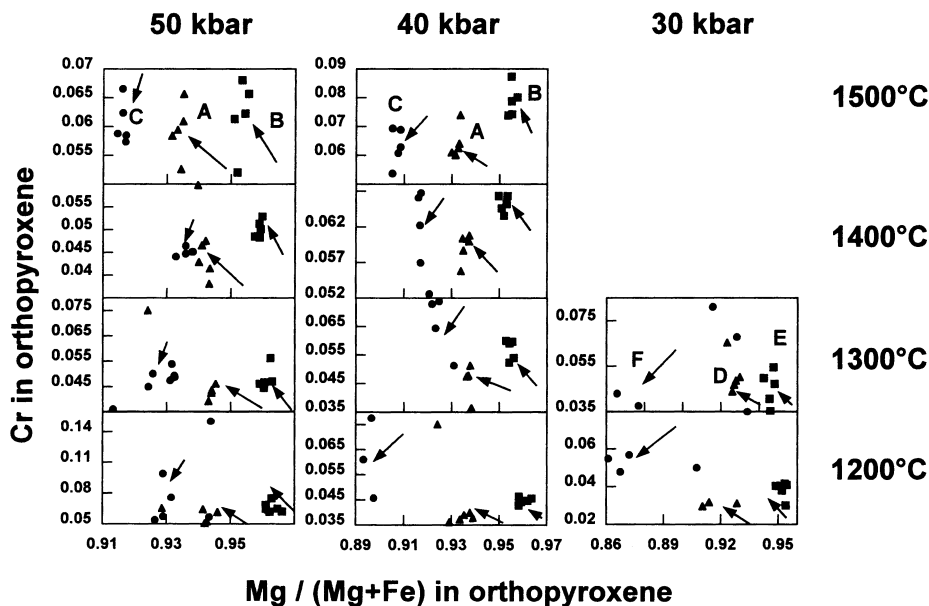


Fig. 5. Al contents of experimental orthopyroxenes (formula units) from harzburgite assemblage at different pressures and temperatures. See Fig. 2 for symbol explanation.

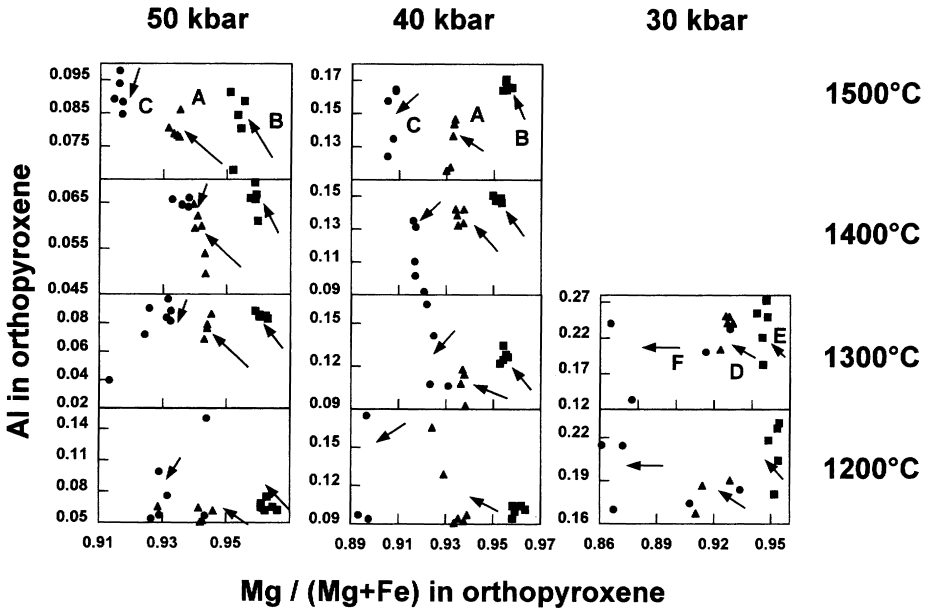


Fig. 6. Cr contents of experimental orthopyroxenes (formula units). See Fig. 2 for symbol explanation.

Al scatter more strongly (Fig. 5, 6). Al and Cr in the experiments with mixtures (B) and (E) are very consistent (within 0.01) in all experiments at 40 kbar and in the majority of the experiments at 50 kbar. At 30 kbar and also at 50 kbar and 1400–1500°C both elements form elongated fields which are located differently relative to the composition of orthopyroxene from the experiments with mixtures (A) and (D) (Fig. 5, 6). The latter plot along a trend that starts at very low Cr and Al contents and extends to overlap with concentrations from experiments with mixtures (B) and (E). Orthopyroxenes from the experiments with initial high-chromium orthopyroxene (mixtures (C) and (F)) show usually the maximum scatter in Cr and Al contents, which overlap both the ranges found in the experiments with other mixtures.

Approach to equilibrium

The use of three different materials with practically identical bulk compositions but different compositions of starting mineral phases was aimed to approach equilibrium state from three directions and ascertain with more confidence the compositions of phases which may be used for further extrapolation and application to thermobarometry. The produced phases in most of the ex-

periments are rather uniform with respect to their $Mg/(Mg+Fe)$ ratio independent of the choice of iron-bearing phases in the starting material. We therefore used the minimum and maximum values found in run products as brackets for the equilibrium values in each experiment.

Several problems arise in the interpretation of our results with respect to Cr-Al distribution. We discuss these here briefly and deal with them more extensively in Part II of this work. The behaviour of $Cr/(Cr+Al)$ ratio is more complicated than was initially expected. One of the complications relates to the instability of highly chromian and aluminous orthopyroxene in starting mixtures (C) and (F) under experimental conditions. Such an orthopyroxene probably reacts with spinel in the early stages of experiments and produces an orthopyroxene with low Al and Cr content plus relatively Cr-poor garnet. Reaction then proceeds from two directions, which results in considerable scatter and little value for using these data to determine equilibrium garnet and orthopyroxene compositions. Changes in garnet composition in the experiments with other mixtures appear to approach equilibrium from two directions: from pure pyrope in the (A) and (D) mixture experiments and from highly chromian garnet gaining alumina from coexisting spinel (Fig. 3).

Only at 50 kbar and 1400 and 1500°C we observe the anticipated trends in orthopyroxene composition from low Al and Cr extending to highest values which are almost the same in the experiments with mixtures (A), (B), (D) and (E) (Fig. 5, 6). At other pressures and temperatures, orthopyroxenes in the experiments with mixtures (B) and (E) are more aluminous than orthopyroxenes from the experiments with initial mixtures (A) and (C). We believe that this results from the instability of high chromium garnet (in starting mixtures (B) and (E)) at low temperature and low pressure. The initial garnet with $Cr/(Cr+Al) = 0.6$ reacts with olivine yielding spinel and Cr-Al rich orthopyroxene, which changes then towards an equilibrium composition with lower Cr and Al.

Molar volumes of minerals

The molar volumes for most of the end-members of olivine, orthopyroxene, garnet and spinel solid solutions are well known, although some discrepancies between reported results still remain (Doroshev *et al.*, 1997). Very little is known about some of the mixing volumes of phases, especially between Cr and Al end-members. We determined mixing volumes of solid solutions produced in the experiments and refined volumes of some end-members.

The bulk compositions of starting mixtures ensured high enough proportions of all minerals in the run products to determine precisely the positions of major reflections of all phases on the X-ray diffraction diagrams. The peaks on the diffraction pictures were usually very well defined and narrow, which allowed us to determine unit-cell parameters with high precision (Tables 2–5). Much higher uncertainty stems from the composition of phases, which show compositional variations, especially in low-temperature experiments. From the very sharp peaks on the X-ray diffraction diagrams we may safely assume that the phase under consideration is rather uniform in composition, and that extreme chemical compositions, as obtained by microprobe, comprise only relatively small volumes. The dominant composition of the mineral must then be similar to the average of microprobe analyses, provided they were taken randomly over the area of the sample. The medians of measured values were used in calculating composition-volume relationships and the variance of microprobe analyses was a

measure for weighting individual volume determinations in further statistical treatment.

The general expression used for the approximation of volume data is:

$$V = V_{\text{ideal}} + V_{\text{ex}} \quad (1)$$

where the expression for excess mixing volume is determined by the adopted mixing model. The ideal term may be specified in several ways because for a multisite solid solution the choice of end-members to express mineral composition is not unique. The volumes of all possible end-members are not necessarily coplanar, so the volume effects of reciprocal reactions must be included into the expression for ideal volume:

$$V_{\text{ideal}} = \sum V_i X_i + \sum \Delta V_{jk} X_j X_k \quad (2)$$

where V_i and X_i are the volumes and mole fraction of selected end-members and ΔV_{jk} is the volume effect of the reciprocal reaction of the formation of the end-members that are not used to express mineral composition (Wood & Nicholls, 1978).

The unknown coefficients of equations 1 and 2 were calculated by the weighted least squares method. The weights of individual measurements were taken as reciprocal variances of the quantity V_{meas} minus linear part of V_{ideal} (Eq. 2):

$$\sigma^2(V_{\text{meas}} - \sum V_i X_i) = \sigma^2(V) + \sum \sigma^2(X_i) V_{i0}^2 \quad (3)$$

where $\sigma^2(V)$ is the variance of the measured volume, $\sigma^2(X_i)$ is the variance of the compositional parameter X_i and V_{i0} is the estimated value of the volume of end-member i . It was found that the first term in this expression in the majority of cases is very small and may be neglected.

Formulation of the excess term in Eq. 1 followed the initial assumption of a multisite solid solution with subregular or regular mixing among components, independently on each site. The choice of the final model which might result in setting some coefficients to zero (*i.e.* assumption of ideal or symmetrical regular model instead of asymmetrical) was based on the value of Student's t statistic at a confidence level of 95%.

In addition to the data from the present work, volumes measured by Doroshev *et al.* (1997) were also included into the data set. In some cases, the molar volumes of pure end-members were used to constrain volume-composition relationships. The volumes of end-members were never fixed even if

Table 6. Average molar volumes of some olivine, spinel, garnet, and orthopyroxene end-members from the literature.

End-member	V (J/mol)	1 σ	Data sources*
Olivine			
Forsterite, Mg ₂ SiO ₄	4.363		2, 3
Fayalite, Fe ₂ SiO ₄	4.635		2, 4
Cr ₂ SiO ₄	4.77		17
Spinel			
Spinel, MgAl ₂ O ₄	3.976	0.004	2, 3, 20, 23
Picrochromite, MgCr ₂ O ₄	4.357	0.002	8, 20, 23
Garnet			
Pyrope, Mg ₃ Al ₂ Si ₃ O ₁₂	11.321	0.007	2, 3, 7, 8, 19
Almandine, Fe ₃ Al ₂ Si ₃ O ₁₂	11.532	0.004	2, 11, 14
Grossular, Ca ₃ Al ₂ Si ₃ O ₁₂	12.534	0.001	7, 15, 16, 19
Knorringite, Mg ₃ Cr ₂ Si ₃ O ₁₂	11.758		21
	11.746		7, 13
Fe ₃ Cr ₂ Si ₃ O ₁₂	11.996		9
Uvarovite, Ca ₃ Cr ₂ Si ₃ O ₁₂	13.01	0.03	12, 18, 24
Orthopyroxene			
Enstatite, Mg ₂ Si ₂ O ₆	6.266	0.005	2, 3, 8
Ferrosilite, Fe ₂ Si ₂ O ₆	6.594	0.004	1, 2, 22
MgAl ₂ SiO ₆	6.2		5, 6
	5.89		10
	5.963		8

* (1) Anovitz *et al.*, 1993; (2) Berman & Aranovich, 1996; (3) Charlut *et al.*, 1975; (4) Chatillon-Colinet *et al.*, 1983; (5) Chatterjee & Terhart, 1985; (6) Danckwerth & Newton, 1978; (7) Doroshev *et al.*, 1990; (8) Doroshev *et al.*, 1997; (9) Fursenko, 1981; (10) Gasparik & Newton, 1984; (11) Geiger *et al.*, 1987; (12) Huckenholz & Kittel, 1975; (13) Irifune *et al.*, 1982; (14) Keesmann *et al.*, 1971; (15) Kozziol & Newton, 1989; (16) Krupka *et al.*, 1979; (17) Li *et al.*, 1995; (18) Naka *et al.*, 1975; (19) Newton *et al.*, 1977; (20) Oka *et al.*, 1984; (21) Ringwood, 1977; (22) Sueno *et al.*, 1976; (23) Webb & Wood, 1986; (24) Wood & Kleppa, 1984.

known to high precision, because small systematic errors could have been misinterpreted in such a case as indicating non-ideal mixing relationships. Average values reported by various authors were used instead as additional data points and their variances were used as weighting factors (Table 6).

Olivine

Nineteen measurements from our experimental products span a range of Mg/(Mg+Fe) ratios from 0.9 to 0.95. This range is too narrow to calibrate excess mixing volume with much confidence. Our measurements are best described by the simple linear relationship with respect to X_{Mg}:

$$V_{ol} = V_{fo}X_{Mg} + V_{fa}(1-X_{Mg}) \quad (4)$$

Extrapolation of this relationship to pure end-members yields molar volumes (J/bar) of V_{fo} = 4.370 ($\sigma = 0.001$) and V_{fa} = 4.672 ($\sigma = 0.018$), which are significantly higher than those reported by other authors (Table 6). The small positive excess mixing volumes for forsterite-fayalite solid solution as proposed by Schwab & Küstner (1977), Berman *et al.* (1995) and Berman & Aranovich (1996) (W_{FeMg}V = 0.01–0.045 J/bar) are too low to be responsible for the discrepancy. The high apparent volumes of olivine in our experiments may result from Cr content in our olivines, because of the high molar volume of Cr₂SiO₄ (Table 6). Concentrations of 0.5 to 2.35 mol.% of Cr₂SiO₄ measured in the experimental olivine (assuming that all chromium is Cr²⁺) are sufficient to explain the difference between our data and other estimates.

Spinel

Neglecting ordering of Fe, Mg, and Al between octahedral and tetrahedral sites, spinel composition may be described by two compositional parameters: X_{Cr} = Cr/(Cr+Al) and X_{Mg} = Mg/(Mg+Fe). We selected chromite, FeCr₂O₄, spinel, MgAl₂O₄, and picrochromite, MgCr₂O₄ as independent end-members. A two-parameter Margules expression was used to describe the non-ideal mixing of di- and trivalent cations. Thus we have for spinel molar volume:

$$V_{Sp} = (1-X_{Mg})V_{Cr} + (1-X_{Cr})V_{Sp} + (X_{Mg} + X_{Cr} - 1)V_{pc} + (1-X_{Mg})(1-X_{Cr})\Delta V_1 + X_{Mg}(1-X_{Mg})[W_{MgFe}^{V}(1-X_{Mg}) + W_{FeMg}^{V}X_{Mg}] + 2X_{Cr}(1-X_{Cr})[W_{CrAl}^{V}(1-X_{Cr}) + W_{AlCr}^{V}X_{Cr}] \quad (5)$$

where ΔV_1 is the volume change of the reciprocal reaction:



The molar volume of (Mg,Fe)(Cr,Al)₂O₄ solid solution depends mainly on Cr/(Cr+Al), while the effect of Mg/(Mg+Fe) is much smaller (Fig. 7). Cr/(Cr+Al) ratios span a wide range, from 0.3 to 0.9, which allows us to constrain mixing parameters with more confidence. The range of Mg/(Mg+Fe) ratio is much smaller (0.65–0.85), resulting in higher relative errors in the calculated excess mixing volumes due to Fe-Mg exchange. Experimental results do not require an asymmetric model of Fe-Mg excess mixing volume, so the respective term in Eq. 5 was reduced to X_{Mg}(1–

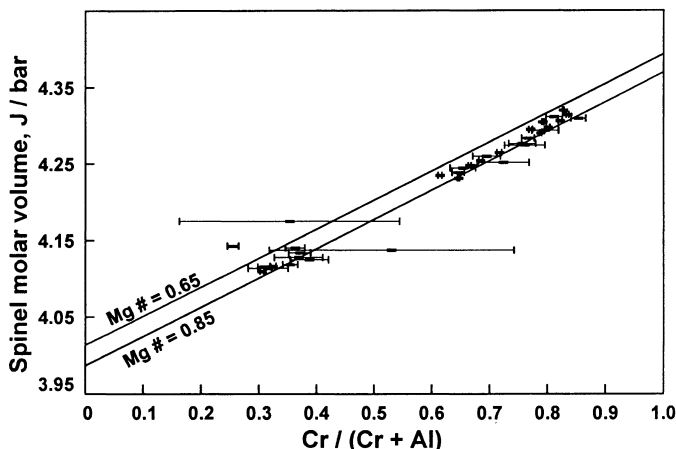


Fig. 7. Dependence of measured spinel molar volume on Cr/(Cr+Al) ratio. Reference lines are calculated assuming linear dependency of molar volume on Cr/(Cr+Al) and Mg# = Mg/(Mg+Fe) ratio. Error bars are one standard deviation. The standard deviation of measured volume is less than the size of symbols.

$X_{Mg}W_{MgFe}^V$. Because of significant uncertainties in the composition of spinel, the extrapolation of our data to pure end-members yielded molar volumes with unsatisfactorily high standard errors and strong correlation with excess-mixing-volume parameters. We therefore included the volume of $MgAl_2O_4$ as an additional data point.

The available volume data for spinel, $MgAl_2O_4$, scatter between 3.974 and 3.981 (Table 6). Doroshev *et al.* (1997) suggested that this scatter stems from significant solubility of Al_2O_3 in spinel at high temperature (Viertel & Seifert, 1979) and obtained a value of 3.974 ± 0.001 J/bar for the molar volume of pure spinel. We used this value for spinel and also the X-ray diffraction data for $MgAl_2O_4$ - $MgCr_2O_4$ solutions from Doroshev *et al.* (1997) to fit the volume-composition relationship, Eq. 5.

In further treatment of the data we found that models with non-zero ΔV_1 yielded very high volumes of $FeCr_2O_4$ (>4.49 J/mol) with large uncertainties ($1\sigma = 0.02$) and strong correlation with the value of ΔV_1 . When ΔV_1 was set to zero errors in

the volumes of pure end-members and residuals in spinel solid solution volume ($1\sigma = 0.005$ J/mol) were much smaller. The calculated volumes of end-members (Table 7) are consistent with data of other authors (Table 6). Small non-linearity was found in the volume of spinel solid solution with respect to both Cr/(Cr+Al) and Mg/(Mg+Fe), indicating non-zero excess mixing volumes. This excess mixing volume is negative at high Cr/(Cr+Al) value and positive in aluminium-rich compositions (Fig. 8). Thus, the results in the FMASCr system confirm the conclusion of Doroshev *et al.* (1997) who obtained an asymmetric model with different signs of Margules volume mixing parameters in iron-free Cr-Al spinels. The values of these parameters as determined by Doroshev *et al.* (1997) ($W_{CrAl} = 0.027$ and $W_{AlCr} = -0.012$ J/bar) are higher but consistent within the 1σ range with the present results (Table 7). The relationship of the spinel molar volumes with Mg/(Mg+Fe) ratio (Fig. 9) indicates negative excess mixing volume between $Mg(Cr,Al)_2O_4$ and $Fe(Cr,Al)_2O_4$ (Table 7).

Table 7. Approximation of spinel molar volume using Margules formulation.

Parameter	Value	1s	Correlation matrix				
			2	3	4	5	6
1 V_{chr}	4.441	0.002	0	0	0.04	-0.006	-0.48
2 V_{sp}	3.975	0.001		-0.01	-0.25	-0.04	0
3 V_{pc}	4.356	0.001			0.15	-0.68	0.28
4 W_{CrAl}^V	0.017	0.009				-0.49	-0.14
5 W_{AlCr}^V	-0.01	0.006					-0.52
6 $W_{FeMg}^V = W_{MgFe}^V$	-0.02	0.007					

37 points, $s(V) = 0.005$

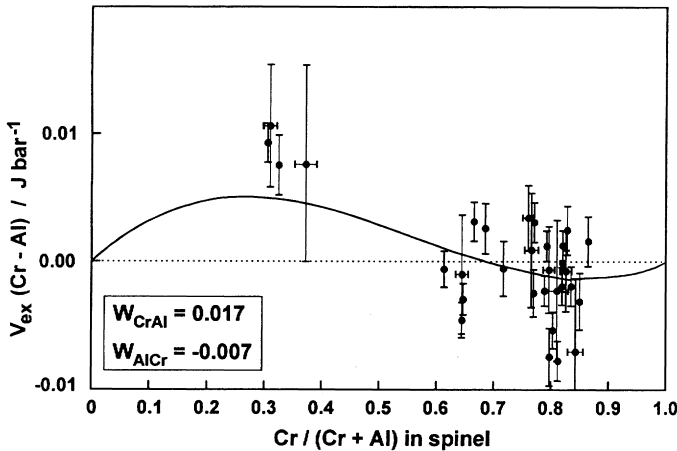


Fig. 8. Calculated excess mixing volume due to Cr-Al exchange in spinels from the experiments in the FMASCr (this work) and MASCr systems (Doroshev *et al.*, 1997). $V_{ex}(\text{Cr-Al}) = V_{ex} - W_{\text{FeMg}}X_{\text{Mg}}(1-X_{\text{Mg}})$. Solid line shows the approximation of spinel molar volume with the asymmetric Margules model. Error bars are one standard deviation.

The *t* test of obtained parameters shows that the values of W^V are significant at 95–97.5 % probability level, except for W_{AlCr}^V , which differs from 0 at a confidence level <90%. Note, however, that the difference $W_{\text{CrAl}}^V - W_{\text{AlCr}}^V$ is greater than 0.01 with a probability of 95 %, thus supporting significant asymmetry of Cr-Al mixing volume in spinel. The obtained volume parameters of spinel are characterised normally by weak mutual correlation (usually, $r \ll 0.5$) (Table 7).

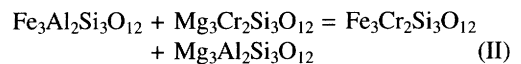
Garnet

Some garnets from our experimental products contain small amounts of calcium ($\text{Ca}/(\text{Ca}+\text{Fe}+\text{Mg})$ up to 0.04), so we considered garnet composition as a two-site solid solution, $(\text{Ca}, \text{Fe}, \text{Mg})_3(\text{Cr}, \text{Al})_2\text{Si}_3\text{O}_{12}$, with independent mixing of di- and trivalent cations. Three independent composition

parameters are necessary to express garnet composition: $X_{\text{Ca}} = \text{Ca}/(\text{Ca}+\text{Fe}+\text{Mg})$, $X_{\text{Mg}} = \text{Mg}/(\text{Ca}+\text{Fe}+\text{Mg})$, and $X_{\text{Cr}} = \text{Cr}/(\text{Cr}+\text{Al})$. The set of independent end-members includes pyrope ($\text{Mg}_2\text{Al}_3\text{Si}_3\text{O}_{12}$), grossular ($\text{Ca}_3\text{Al}_2\text{Si}_3\text{O}_{12}$), knorringite ($\text{Mg}_3\text{Cr}_2\text{Si}_3\text{O}_{12}$) and almandine ($\text{Fe}_3\text{Al}_2\text{Si}_3\text{O}_{12}$). The molar volume of garnet solid solution may then be expressed as:

$$V^{\text{Grt}} = (X_{\text{Mg}}-X_{\text{Cr}})V_{\text{pyr}} + X_{\text{Ca}}V_{\text{gr}} + X_{\text{Cr}}V_{\text{kn}} + (1-X_{\text{Mg}}-X_{\text{Ca}})V_{\text{alm}} + (1-X_{\text{Mg}}-X_{\text{Ca}})X_{\text{Cr}}\Delta V_{\text{II}} + X_{\text{Ca}}X_{\text{Cr}}\Delta V_{\text{III}} + V_{\text{Ca-Mg-Fe}}^{\text{ex}} + V_{\text{Cr-Al}}^{\text{ex}} \quad (6)$$

where ΔV_{II} and ΔV_{III} are the volume changes of reciprocal reactions:



and

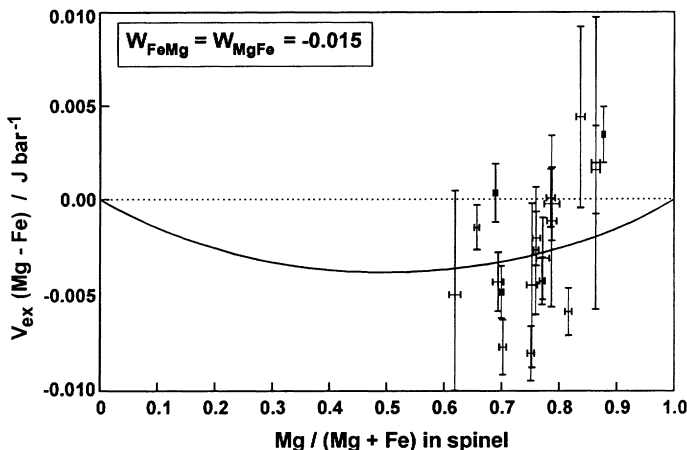


Fig. 9. Calculated excess mixing volume due to Fe-Mg exchange in spinels from the experiments in the FMASCr system. $V_{ex}(\text{Fe-Mg}) = V_{ex} - 2X_{\text{Cr}}(1-X_{\text{Cr}})[W_{\text{CrAl}} + X_{\text{Cr}}(W_{\text{AlCr}}-W_{\text{CrAl}})]$. Solid line shows the approximation of spinel molar volume with the symmetric Margules model. Error bars are one standard deviation.

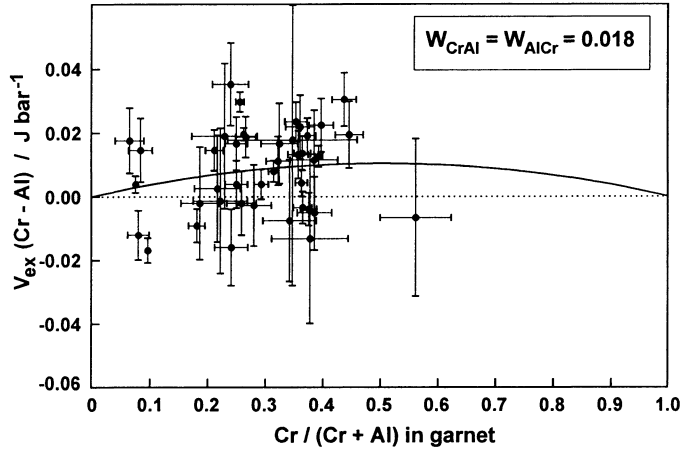
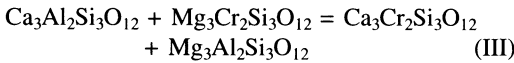


Fig. 10. Excess garnet mixing volume due to Cr-Al exchange calculated for experimental garnets from FMASCr (this work) and MASCr (Doroshev *et al.*, 1997) systems. Symmetrical and asymmetrical models approximate the deviation from ideal mixing with the same precision. Error bars are one standard deviation.



and $V_{\text{Ca-Mg-Fe}}^{\text{ex}}$ and $V_{\text{Cr-Al}}^{\text{ex}}$ are the excess mixing volumes with respect to Fe-Mg-Ca and Al-Cr substitution in garnet.

Similar to spinel, the scatter of measured garnet compositions is too high to allow all the coefficients of Eq. 6 to be determined with confidence without additional constraints. Considerable efforts were undertaken in the last decades to determine volume properties of garnet solid solution, both from direct measurement and from phase equilibrium data. We used average values from the literature for pyrope, almandine and grossular (Table 6). Much more uncertainty is related to the molar volume of the knorringite end-member (Table 6). We accepted the value of Doroshev *et al.* (1997) assigning a rather large uncertainty (± 0.01 J/bar) and, consequently, low weight to this point. Molar volumes of $\text{Fe}_3\text{Cr}_2\text{Si}_3\text{O}_{12}$ and uvarovite (Table 6) were used to constrain the vol-

ume changes of reciprocal reactions (II) and (III): $\Delta V_{\text{II}} = 0.037 \pm 0.015$ and $\Delta V_{\text{III}} = 0.04 \pm 0.03$ J/bar.

The volume mixing properties of aluminous garnets have been repeatedly studied (*e.g.* Wood, 1988; Geiger *et al.*, 1987; Koziol & Newton, 1989). We used the generalised Margules equation derived by Berman & Brown (1984) and Berman (1988) and the model parameters obtained by Berman & Aranovich (1996) to account for the non-ideal Fe-Mg-Ca mixing in garnet solid solution. There are few data on mixing volumes of Cr-Al garnets. Huckenholz & Knittel (1975) and Wood & Kleppa (1984) observed linear volume-composition relations in grossular-uvarovite solid solutions. Doroshev *et al.* (1997) did not find any significant deviation from ideal mixing in the pyrope-knorringite join, but noted large scatter in their data. Cr-Al mixing in garnet solid solution is expressed in terms of the asymmetric Margules model:

$$V_{\text{Cr-Al}}^{\text{ex}} = 2X_{\text{Cr}}(1-X_{\text{Cr}})[W_{\text{AlCr}}^{\text{V}}X_{\text{Cr}} + W_{\text{CrAl}}^{\text{V}}(1-X_{\text{Cr}})] \quad (7)$$

Table 8. Approximation of garnet molar volume using Margules formulation.

Parameter	Value	1σ (J/bar)	Correlation matrix					
			2	3	4	5	6	7
1 V_{pyr}	11.32	0.003	0	0.20	-0.24	0.11	0.07	-0.62
2 V_{gr}	12.53	0.004		0	0	0	-0.1	0
3 V_{kn}	11.75	0.01			0.03	-0.62	-0.95	-0.82
4 V_{alm}	11.54	0.005				-0.40	-0.10	0.04
5 ΔV_{II}	0.03	0.02					0.65	0.40
6 ΔV_{III}	0.04	0.01						0.65
7 $W_{\text{AlCr}}^{\text{V}} = W_{\text{CrAl}}^{\text{V}}$	0.018	0.007						

55 points, $\sigma(V) = 0.012$

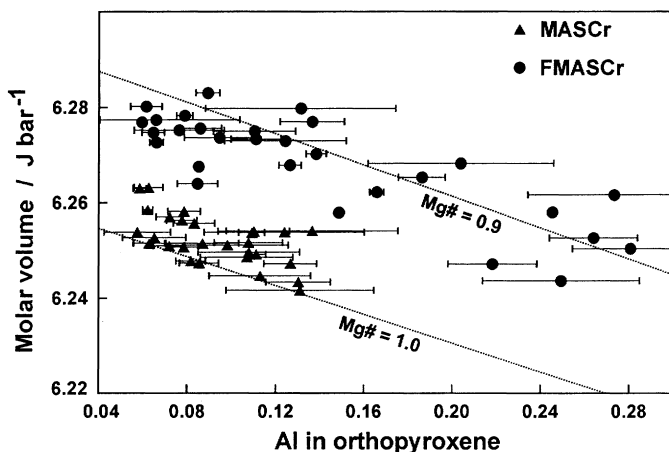


Fig. 11. Measured molar volumes of experimental orthopyroxenes from the MASCr (Doroshev *et al.*, 1997) and FMASCr (this work) systems. Dashed lines show ideal volumes for $(\text{Mg,Fe})_2\text{Si}_2\text{O}_6 - (\text{Mg,Fe})\text{AlAlSiO}_6$ mixtures at $\text{Mg}\# = \text{Mg}/(\text{Mg}+\text{Fe}) = 1.0$ and 0.9. Error bars are one standard deviation.

We used our data together with the results of Doroshev *et al.* (1997) for the iron-free system and the pure end-member volumes (Table 6) to have a total set of 60 points, from which 5 points were rejected during computation on the basis of the 3σ criterion. The remaining data for molar volumes may be fitted by a symmetrical ($W_{\text{AlCr}}^V = W_{\text{CrAl}}^V = 0.018 \text{ J/bar}$) mixing model (Table 8, Fig. 10). Introduction of the second Margules parameter does not significantly improve the fit. The resulting molar volumes for the end-members and reciprocal reactions are within the ranges reported in the literature (Table 6). The value obtained for pure knorringite is intermediate between those of Ringwood (1977) and Doroshev *et al.* (1997). However, large uncertainty of V_{kn} ($1\sigma = 0.01 \text{ J/bar}$) is of the same magnitude as the maximum difference between the values of V_{kn} reported by different authors. Moreover, the molar volume of knorringite correlates strongly with the volume changes of the reciprocal reactions (Table 8). This implies that these parameters may change considerably if new data points will be added. Thus, our results are compatible with both the maximum and minimum values of V_{kn} from the literature. More precise experimental data are certainly needed to resolve this problem.

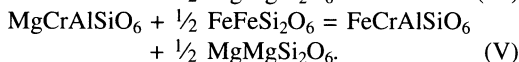
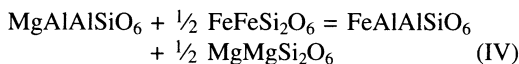
Orthopyroxene

Solid solutions of orthorhombic pyroxene show mixing on one tetrahedral and two octahedral sites. In the FMASCr system orthopyroxene composition may be expressed by the structural for-

mula $(\text{Mg, Fe})^{\text{M}2}(\text{Mg, Fe, Al, Cr})^{\text{M}1}(\text{Si, Al, Cr})^{\text{T}}\text{O}_6$, suggesting that Cr and Al enter orthopyroxene structure *via* heterovalent isomorphism $(\text{Al,Cr})_2 \leftrightarrow \text{MgSi}$. Another substitution scheme, $(\text{Al,Cr}) \leftrightarrow \text{Mg}_{1.5}$ results in the formation of cation-deficient pyroxene and is realised only in silica-saturated systems (Gasparik, 1984; Malinovskaya *et al.*, 1991). The complete formulation of orthopyroxene solid solution should account for the non-random distribution of cations between sites and non-ideal mixing on individual sites, which results in rather complicated models (*e.g.* Sack & Ghiorso, 1994). Given the insufficient data on Cr in orthopyroxene, we proposed a simplified model based on two assumptions.

We assumed that Cr occurs only in octahedral positions of orthopyroxene structure. In the Al-deficient region Cr can enter tetrahedral positions as well (Ikeda & Yagi, 1977), but the large size of Cr^{3+} ion suggests its strong preference for octahedral sites. This is compatible with the fact that in our experimental orthopyroxenes Al always prevails over Cr (Fig. 4). In addition, we ignored cation ordering assuming random Fe and Mg distribution between M1 and M2 sites.

Assuming the ideal charge-balanced stoichiometry, the composition of orthopyroxene may be described by three independent parameters: $X_{\text{Mg}} = \text{Mg}/(\text{Mg}+\text{Fe})$, $X_{\text{Al}}^{\text{M}1} = (\text{Al}-\text{Cr})/2$, and $X_{\text{Cr}}^{\text{M}1} = \text{Cr}$ (cations in structural formula based on 6 oxygens). Enstatite ($\text{MgMgSi}_2\text{O}_6$), ferrosilite ($\text{FeFeSi}_2\text{O}_6$), MgAlAlSiO_6 and MgCrAlSiO_6 were used as independent end-members. The formation of iron-bearing chromian and aluminous molecules is specified by two reciprocal reactions:



The molar volume of orthopyroxene solid solution is given by:

$$\begin{aligned} V^{\text{opx}} = & X_{\text{Al}}^{\text{M1}} V_{\text{ts}} + X_{\text{Cr}}^{\text{M1}} V_{\text{CrtS}} + (1 - X_{\text{Al}}^{\text{M1}} X_{\text{Cr}}^{\text{M1}}) \\ & (1 - X_{\text{Mg}}) V_{\text{fs}} + (1 - X_{\text{Al}}^{\text{M1}} - X_{\text{Cr}}^{\text{M1}}) X_{\text{Mg}} V_{\text{en}} \\ & + \Delta V_{\text{IV}} X_{\text{Al}}^{\text{M1}} (1 - X_{\text{Mg}}) + \Delta V_{\text{V}} X_{\text{Cr}}^{\text{M1}} (1 - X_{\text{Mg}}) + V^{\text{ex}} \end{aligned} \quad (8)$$

Two factors complicate the determination of orthopyroxene mixing volume parameters. The first is the narrow range of orthopyroxene compositions (especially in Cr) and the second is large scatter in $X_{\text{Cr}}^{\text{M1}}$ and $X_{\text{Al}}^{\text{M1}}$ in individual experiments. Unfortunately, the scatter is especially large in low-pressure orthopyroxenes, which are highest in Al. This fact hampers precise determination of the volume of Al orthopyroxene. The molar volume of experimental pyroxenes ranges from 6.24 to 6.28 J/bar and depends on X_{Mg} and Al content (Fig. 11). Data from this work together with those of Doroshev *et al.* (1997) for the MASCr system were used to calculate the parameters of Eq. 8 (62 data points). No data for the end-members were included. Taking into account the uncertainties in compositions, the best approximation of orthopyroxene molar volume was obtained with an ideal linear mixing of the four end-members, *i.e.* at $\Delta V_{\text{IV}} = \Delta V_{\text{V}} = V^{\text{ex}} = 0$ (Table 9). Incorporation of either of these parameters into the model increased the residuals, while Student's *t* statistics of calculated values was always less than 1.

The calculated molar volume of enstatite (Table 9) is practically identical to that reported by other researchers (Table 6). Other end-member molar volumes are obtained by extrapolating over a considerable compositional interval and have much higher standard errors (Table 9). Our value for ferrosilite molar volume is higher than that reported by other authors (Table 6), but the difference is comparable with the calculated standard deviation. Danckwerth & Newton (1978) and Chatterjee & Terhart (1985) suggested large negative non-ideality for the mixing volume in the MgAlAlSiO_6 - $\text{Mg}_2\text{Si}_2\text{O}_6$ binary and the high molar volume of MgAlAlSiO_6 (6.2 J/bar), whereas Gasparik & Newton (1984) and Doroshev *et al.* (1997) reported lower volumes (5.89 and 5.963 J/bar, respectively) and near-ideal mixing in this join. Our value (6.035 J/bar) is substantially lower

Table 9. Approximation of orthopyroxene molar volume using Margules formulation.

Parameter	Value 1σ		Correlation matrix		
	(J/bar)		2	3	4
1 V_{ts}	6.04	0.02	-0.41	-0.34	0.33
2 V_{CrtS}	6.14	0.03		0.30	-0.89
3 V_{fs}	6.61	0.02			-0.59
4 V_{en}	6.266	0.002			

62 points, $\sigma(V) = 0.003$

than that of Danckwerth & Newton (1978), but higher than the values reported by Gasparik & Newton (1984) and Doroshev *et al.* (1997). As far as direct measurement is not possible, the extrapolation of volume data to pure MgAlAlSiO_6 depends strongly on the accepted mixing model and the range of composition. Our results do not support high excess mixing volumes of Mg-Al orthopyroxenes, although in our multicomponent orthopyroxenes non-idealities in different binaries may cancel each other and yield negligible total excess mixing volumes. However, Fe-Mg mixing in orthopyroxene is probably close to ideal (*e.g.* Berman & Aranovich, 1996) and the excess mixing volume in Mg-Al and Mg-Cr pyroxenes could hardly be large and of opposite signs. Thus, it is more probable that the volumes of (Mg, Fe)(Al, Cr)(Si, Al)₂O₆ orthopyroxenes are close to the ideal model.

The zero values of the volume changes of reciprocal reactions IV and V imply that the molar volumes of FeAlAlSiO_6 and FeCrAlSiO_6 are coplanar, within the uncertainties, with those of the selected independent end-members, and may be calculated as:

$$V_{\text{Fets}} = V_{\text{ts}} + \frac{1}{2} V_{\text{fs}} - \frac{1}{2} V_{\text{en}} = 6.21 \pm 0.02 \text{ J/bar}$$

and

$$V_{\text{Fe-CrtS}} = V_{\text{CrtS}} + \frac{1}{2} V_{\text{fs}} - \frac{1}{2} V_{\text{en}} = 6.3 \pm 0.03 \text{ J/bar.}$$

Conclusions

Our experimental results show low rate of equilibration with respect to Cr-Al exchange in orthopyroxene, garnet, and spinel. This resulted in considerable scatter in their composition even at the highest temperature (1500°C). The inhomogeneity of phases, primarily, garnet and orthopyroxene, hampered the precise determination of mixing volumes, hence some parameters were derived

with considerable uncertainty. The main result obtained in this study is the small deviations from ideality in Cr-Al mixing volumes in all phases investigated. The maximum non-ideality associated with Cr-Al mixing in both garnet and spinel does not exceed 0.01 ± 0.01 J/bar. The contribution of such effects is energetically important only at very high pressures (e.g. > 50 kbar). An asymmetric deviation from ideal mixing volume was noted in spinel Cr-Al mixing, confirming the results of Doroshev *et al.* (1997). Because of the asymmetry of the excess mixing volume, spinel volumes are almost ideal at high Cr/(Cr+Al) ratios, typical of high-pressure mantle parageneses. Some non-ideality is related also to Fe-Mg mixing of spinel, but the magnitude of this effect is even smaller than along the Cr-Al join. More important is the non-ideality of garnet volumes because at pressures of 50–70 kbar its Cr/(Cr+Al) ratio in equilibrium with spinel, olivine, and orthopyroxene is close to 0.5, where the maximum effect of non-ideal mixing is expected. Considerable uncertainties remain in the mixing volumes and the volumes of some end-members of orthopyroxene. The non-ideality associated with Cr-Al-Fe-Mg mixing is probably also small. Moreover, at high pressures Al content of orthopyroxene is very low, thus the contribution of excess mixing volume becomes small in any case and does not influence significantly equilibria between phases.

Acknowledgements: We are grateful to M. Engi and an anonymous reviewer for very helpful comments and suggestions. The work was financially supported by the Deutsche Forschungsgemeinschaft (DFG) and Russian Foundation for Basic Research.

References

- Anovitz, L.M., Essene, E.J., Metz, G.W., Bohlen, S.R., Westrum Jr., E.F., Hemingway, B.S. (1993): Heat capacity and phase equilibria of almandine, $\text{Fe}_3\text{Al}_2\text{Si}_3\text{O}_{12}$. *Geochim. Cosmochim. Acta*, **57**, 4191-4204.
- Berman, R.G. (1988): Internally-consistent thermodynamic data for minerals in the system $\text{Na}_2\text{O-K}_2\text{O-CaO-MgO-FeO-Fe}_2\text{O}_3\text{-Al}_2\text{O}_3\text{-SiO}_2\text{-TiO}_2\text{-H}_2\text{O-CO}_2$. *J. Petrol.*, **29**, 445-522.
- Berman, R.G. & Aranovich, L.Y. (1996): Optimized standard state and mixing properties of minerals: I. Model calibration for olivine, orthopyroxene, cordierite, garnet, and ilmenite in the system $\text{FeO-MgO-CaO-Al}_2\text{O}_3\text{-TiO}_2\text{-SiO}_2$. *Contrib. Mineral. Petrol.*, **126**, 1-24.
- Berman, R.G., Aranovich, L.Y., Pattison, D.R.M. (1995): Reassessment of the garnet-clinopyroxene Fe-Mg exchange thermometer: II. Thermodynamic analysis. *Contrib. Mineral. Petrol.*, **119**, 30-42.
- Berman, R.G. & Brown, T.H. (1984): A thermodynamic model for multicomponent melts, with application to the system $\text{CaO-Al}_2\text{O}_3\text{-SiO}_2$. *Geochim. Cosmochim. Acta*, **48**, 661-678.
- Brey, G.P., Weber, R., Nickel, K.G. (1990): Calibration of a belt apparatus to 1800°C and 6 GPa. *J. Geophys. Res.*, **95**, 15603-15610.
- Charlu, T.V., Newton, R.C., Kleppa, O.J. (1975): Enthalpies of formation at 970 K of compounds in the system $\text{MgO-Al}_2\text{O}_3\text{-SiO}_2$ from high temperature solution calorimetry. *Geochim. Cosmochim. Acta*, **39**, 1487-1497.
- Chatillon-Colinet, C., Kleppa, O.J., Newton, R.C., Perkins, III D. (1983): Enthalpy of formation of $\text{Fe}_3\text{Al}_2\text{Si}_3\text{O}_{12}$ (almandine) by high temperature alkali borate solution calorimetry. *Geochim. Cosmochim. Acta*, **47**, 439-444.
- Chatterjee, N.D. & Terhart, L. (1985): Thermodynamic calculation of peridotite phase relations in the system $\text{MgO-Al}_2\text{O}_3\text{-SiO}_2\text{-Cr}_2\text{O}_3$, with some geological applications. *Contrib. Mineral. Petrol.*, **89**, 273-284.
- Danckwerth, P.A. & Newton, R.C. (1978): Experimental determination of the spinel peridotite to garnet peridotite reaction in the system $\text{MgO-Al}_2\text{O}_3\text{-SiO}_2$ in the range 900–1100°C and Al_2O_3 isopleths of enstatite in the spinel field. *Contrib. Mineral. Petrol.*, **66**, 189-201.
- Doroshev, A.M., Brey, G.P., Girmis, A.V., Turkin, A.I., Kogarko, L.N. (1997): Pyrope-knorringite garnets in the Earth's mantle: Experiments in the $\text{MgO-Al}_2\text{O}_3\text{-SiO}_2\text{-Cr}_2\text{O}_3$ system. *Russian Geol. Geophys.*, **38**, 559-586.
- Doroshev, A.M., Galkin, V.M., Turkin, A.I., Kalinin, A.A. (1990): Thermal expansion in the pyrope-grossular and pyrope-knorringite garnet series. *Geochem. Intern.*, **27**, 144-147.
- Engi, M. (1983): Equilibria involving Al-Cr spinels: Fe-Mg exchange with olivine. Experiments, thermodynamic analysis, and consequences for geothermometry. *Am. J. Sci.*, **283A**, 29-71.
- Fursenko, B.A. (1981): Synthesis of new high pressure garnets: $\text{Mn}_3\text{Cr}_2\text{Si}_3\text{O}_{12}$ and $\text{Fe}_3\text{Cr}_2\text{Si}_3\text{O}_{12}$. *Bull. Minéral.*, **104**, 418-422.
- Gasparik, T. (1984): Experimental study of subsolidus phase relations and mixing properties of pyroxene in the system $\text{CaO-Al}_2\text{O}_3\text{-SiO}_2$. *Geochim. Cosmochim. Acta*, **48**, 2537-2545.
- Gasparik, T. & Newton, R.C. (1984): The reversed alumina contents of orthopyroxene in equilibrium with spinel and forsterite in the system $\text{MgO-Al}_2\text{O}_3\text{-SiO}_2$. *Contrib. Mineral. Petrol.*, **85**, 186-196.
- Geiger, C.A., Newton, R.C., Kleppa, O.J. (1987): Enthalpy of mixing of synthetic almandine-grossular and almandine-pyrope garnets from high-temperature solution calorimetry. *Geochim. Cosmochim. Acta*, **51**, 1755-1763.

- Huckenholz, H.G. & Knittel, U. (1975): Stability of grossularite-uvarovite solid solutions. *Contrib. Mineral. Petrol.*, **49**, 211-232.
- Ikeda, K. & Yagi, K. (1977): Experimental study on the phase equilibria in the join $\text{CaMgSi}_2\text{O}_6$ - CaCrSiO_6 with special reference to the blue diopside. *Contrib. Mineral. Petrol.*, **61**, 91-106.
- Irifune, T. & Hariya, T. (1983): Phase relationships in the system $\text{Mg}_3\text{Al}_2\text{Si}_3\text{O}_{12}$ - $\text{Mg}_3\text{Cr}_2\text{Si}_3\text{O}_{12}$ at high pressure and some mineralogical properties of synthetic garnet solid solutions. *Mineral. J.*, **11**, 269-281.
- Irifune, T., Ohtani, E., Kumazawa, M. (1982): Stability field of khorringite $\text{Mg}_3\text{Cr}_2\text{Si}_3\text{O}_{12}$ at high pressure and its implication for the occurrence of Cr-rich pyrope in the upper mantle. *Phys. Earth Planet. Inter.*, **27**, 263-272.
- Keessmann, I., Matthes, S., Schreyer, W., Seifert, F. (1971): Stability of almandine in the system FeO - (Fe_2O_3) - Al_2O_3 - SiO_2 - (H_2O) at elevated pressures. *Contrib. Mineral. Petrol.*, **31**, 132-144.
- Kozioł, A.M. & Newton, R.C. (1989): Grossular activity-composition relationships in ternary garnets determined by reversed displaced-equilibrium experiments. *Contrib. Mineral. Petrol.*, **103**, 423-433.
- Krupka, K.M., Robie, R.A., Hemingway, B.S. (1979): High-temperature heat capacities of corundum, periclase, anorthite, $\text{CaAl}_2\text{Si}_2\text{O}_8$ glass, muscovite, pyrophyllite, KAlSi_3O_8 glass, grossular, and $\text{NaAlSi}_3\text{O}_8$ glass. *Am. Mineral.*, **64**, 86-101.
- Li, J.-P., O'Neill, H.S.C., Seifert, F. (1995): Subsolidus phase relations in the system MgO - SiO_2 - Cr - O in equilibrium with metallic Cr, and their significance for the petrochemistry of chromium. *J. Petrol.*, **36**, 107-132.
- Malinovskaya, E.K., Doroshev, A.M., Bulatov, V.K., Brey, G.P. (1991): Clinopyroxenes of $\text{CaMgSi}_2\text{O}_6$ - $\text{CaAl}_2\text{SiO}_6$ - $\text{Ca}_{0.5}\text{AlSi}_2\text{O}_6$ series in association with anorthite, quartz, coesite and garnet. *Geokhimiya*, **2**, 216-226.
- Meyer, H.O.A. (1975): Chromium and the genesis of diamond. *Geochim. Cosmochim. Acta*, **39**, 929-936.
- Naka, S., Suwa, U., Kameyama, T. (1975): Solid solubility between uvarovite and spessartite. *Am. Mineral.*, **60**, 418-422.
- Newton, R.C., Charlu, T.V., Kleppa, O.J. (1977): Thermochemistry of high pressure garnets and clinopyroxenes in the system CaO - MgO - Al_2O_3 - SiO_2 . *Geochim. Cosmochim. Acta*, **41**, 369-377.
- Nickel, K.G. (1986): Phase equilibria in the system SiO_2 - MgO - Al_2O_3 - CaO - Cr_2O_3 (SMACCR) and their bearing on spinel/garnet lherzolite relationships. *N. Jb. Mineral. Abh.*, **155**, 259-287.
- Nixon, P.H. & Hornung, G. (1968): A new chromium garnet end member, knorringite from kimberlite. *Am. Mineral.*, **53**, 1833-1840.
- Oka, Y., Steinke, P., Chatterjee, N.D. (1984): Thermodynamic mixing properties of $\text{Mg}(\text{Al}, \text{Cr})_2\text{O}_3$ spinel crystalline solution at high temperatures and pressures. *Contrib. Mineral. Petrol.*, **87**, 196-204.
- Reed, S.J.B. & Ware, N.G. (1975): Quantitative electron microprobe analysis of silicates using energy-dispersive X-ray spectrometry. *J. Petrol.*, **16**, 499-519.
- Ringwood, A.E. (1977): Synthesis of pyrope-khorringite solid solution series. *Earth Planet. Sci. Lett.*, **36**, 443-448.
- Sack, R.O. & Ghiorso, M.S. (1994): Thermodynamics of multicomponent pyroxenes: I. Formulation of a general model. *Contrib. Mineral. Petrol.*, **116**, 277-286.
- Schwab, R.G. & Küstner, D. (1977): Präzisionsgitterkonstantenbestimmung zur Festlegung röntgenographischer Bestimmungskurven für synthetischen Olivin der Mischkristallreihe Forsterit-Fayalit. *N. Jb. Mineral. Monatsh.*, **1977**, 205-215.
- Sobolev, N.V. (1974): Deep-seated inclusions in kimberlites and the problem of the composition of the upper mantle. Boyd, F.R. & Brown, D.A. (Eds.), *Am. Geophys. Union, Washington D.C.*, 279 p.
- Stachel, T. & Harris, J.W. (1997): Syngenetic inclusions in diamond from the Birim Field (Ghana) - a deep peridotitic profile with a history of depletion and re-enrichment. *Contrib. Mineral. Petrol.*, **127**, 336-352.
- Sueno, S., Cameron, M., Prewitt, C.T. (1976): Orthoferrosilite: High-temperature crystal chemistry. *Am. Mineral.*, **61**, 38-53.
- Thompson, R.N. & Kushiro, I. (1972): The oxygen fugacity within graphite capsules in the piston-cylinder apparatus at high pressures. *Carnegie Inst. Wash. Yearb.*, **71**, 615-616.
- Turkin, A.I., Doroshev, A.M., Malinovsky, I.Y. (1983): High-pressure and high-temperature investigation of the phases from garnet-bearing associations in the system MgO - Al_2O_3 - Cr_2O_3 - SiO_2 . In "Silicate Systems under High Pressures", Novosibirsk, *Bull. Inst. Geol. Geophys.*, 5-24 (in Russian).
- Viertel, H.U. & Seifert, F. (1979): Physical properties of defect spinels in the system MgAl_2O_4 - Al_2O_3 . *N. Jb. Mineral. Abh.*, **134**, 167-182.
- Webb, S.A.C. & Wood, B.J. (1986): Spinel-pyroxene-garnet relationships and their dependence on Cr/Al ratio. *Contrib. Mineral. Petrol.*, **92**, 471-480.
- Woermann, E. & Rosenhauer, M. (1985): Fluid phase and the redox state of the Earth's mantle. Extrapolations based on experimental, phase-theoretical and petrological data. *Fortschr. Mineral.*, **63**, 263-349.
- Wood, B.J. (1988): Activity measurements and excess entropy-volume relationships for pyrope-grossular garnets. *J. Geol.*, **96**, 721-729.
- Wood, B.J. & Kleppa, O.J. (1984): Chromium-aluminum mixing in garnet: A thermochemical study. *Geochim. Cosmochim. Acta*, **48**, 1373-1375.
- Wood, B.J. & Nicholls, J. (1978): The thermodynamic properties of reciprocal solid solutions. *Contrib. Mineral. Petrol.*, **66**, 389-400.

Received 6 May 1997

Modified version received 7 December 1998

Accepted 3 March 1999

